Automatic, calibration-free quantification of cortical bone porosity and geometry in postmenopausal osteoporosis from ultrashort echo time

Brandon C. Jones, Felix W. Wehrli, Nada Kamona, Rajiv S. Dehspande, Brian-Tinh Duc Vu, Hee Kwon Song, Hyunyeol Lee, Rasleen Grewal, Trevor Chan, Walter Witschey, Matthew MacLean, Nicholas Josselyn, Srikant Iyer, Mona al Mukaddam, Peter J. Snyder, Chamith S. Rajapakse

Penn
UNIVERSITY of PENNSYLVANIA

Background

Clinical Assessment of Osteoporosis (OP)

- From 1990-2019, there was a 33% increase in bone fractures, and a 65% increase in fracture-related disability[1]
- Clinical diagnosis of OP is made via DXA, or Dual-energy X-ray absorptiometry
- DXA has high specificity, but it suffers from very low sensitivity for predicting osteoporotic fracture[2]
- DXA cannot differentiate trabecular bone from cortical bone (CB), nor can it measure bone material properties, which are the chief determinants of bone strength[3,4]

Cortical Bone Imaging

- Osteoporosis medications are known to affect the cortical and trabecular compartments differently[5]
- CB contains ultrashort T_2^* species: (1) Bound water (T_2^* = 390 μs)[7] and (2) Pore water/lipid (T_2^* = 1-1000 ms)[8]

In a prospective study of 7,000 participants, imaging assessment of cortical bone porosity and geometry were predictive of fracture independent of age, sex, height, weight, and BMD[6]

Solid-state MRI (SS-MRI) enables acquisition of previously undetectable ultrashort T_2^* species, thus, enabling quantitative assessment of cortical bone microstructure (porosity).

Cortical Bone Porosity → Pore Water (mol / L); Suppression Ratio

Cortical Bone Geometry → Cortical Thickness; Cortical Area Fraction

However, analysis requires accurate segmentation of periosteum and endosteum which is very time consuming (~80 minutes per scan).

Purpose:

(1) Develop a deep learning model to automatically segment the tibia
(2) Validate the automatically-derived biomarkers of cortical porosity and geometry compared to age, osteoporotic status, and BMD

Study Design and Methods

Bone Water Quantification

$$C_{bone} = C_{ref}\frac{I_{bone}\times F_{ref}}{I_{ref}\times F_{bone}} \times e^{-TE\left(\frac{1}{T_{2,ref}^*}-\frac{1}{T_{2,bone}^*}\right)}$$

Bone signal is calibrated via reference sample

C is the molar concentration (moles/L), I is the image intensity, and F is a mapping function for the fraction of magnetization when RF duration is comparable to T_2^* [7,9]

Suppression Ratio Quantification

$$\frac{S_{unsuppressed}}{S_{suppressed}} = \frac{S_{UTE}}{S_{IR-UTE}} \approx \frac{Pore + Bound}{Bound}$$

- Porous bone will have more pore water and less bound water, corresponding to greater Suppression Ratio[10]
- Larger pores have longer T_2, which improves the efficacy of the adiabatic Inversion Recovery long-T_2 suppression (IR-rUTE), which further increases Suppression Ratio[10]

Training and Test Dataset

Training data: 48 scans (*46 slices) = 2208 slices
Validation data: 7 scans (*46 slices) = 322 slices
Test data: 28 scans (*46 slices) = 1288 slices

EXTERNAL VALIDATION DATASET DEMOGRAPHICS	Number of Subjects	Age (years)	Height (m)	Weight (kg)	BMI (kg/m²)	DXA T-Scores Femoral Neck	Total Hip	Total Lumbar
Young, Healthy	10	27 ± 2	1.7 ± 0.1	65 ± 15	21.7 ± 6.2			
Postmenopausal, Non-Osteoporotic	9	63 ± 6	1.6 ± 0.1	73 ± 11	27.0 ± 4.3	-0.93 ± 0.91	-0.44 ± 0.94	-0.49 ± 1.24
Postmenopausal, Osteoporotic	9	63 ± 6	1.7 ± 0.1	62 ± 9	22. ± 2.1	-2.02 ± 0.65	-1.66 ± 0.43	-2.68 ± 0.59

Conclusion

- Deep learning enables fast, accurate segmentation of cortical bone
  - Segmentation failures were attributed to scanning errors and not model errors
- Automated biomarkers detected osteoporosis-related impairments in cortical porosity and geometry
- Suppression Ratio biomarker enables calibration-free quantification of cortical porosity in vivo

Acknowledgements

NIH R01 AR50068, T32 EB020087, F31 AR079925

References

1. Wu, et al, Global, regional, and national burden of bone fractures in 204 countries and territories, 2021. **2.** Bolotin, H.H., The significant effects of bone structure on inherent patient-specific DXA in vivo bone mineral density measurement inaccuracies. 2004. **3.** Bouxsein, M.L., Technology insight: noninvasive assessment of bone strength in osteoporosis. 2008. **4.** Seeman, E, Bone quality-the material and structural basis of bone strength and fragility. 2006. **5.** Samelson, E.J., Cortical and trabecular bone microarchitecture as an independent predictor of incident fracture risk. 2019. **6.** Kanis, J.A., European guidance for the diagnosis and management of osteoporosis in postmenopausal women. 2019. **7.** Zhao, X., et al, Feasibility of assessing bone matrix and mineral properties in vivo by combined solid-state 1H and 31P MRI. 2017. **8.** Rad, H.S., et al, Quantifying cortical bone water in vivo by three-dimensional ultra-short echo-time MRI. 2011. **9.** Techawiboonwong, A., et al, Cortical Bone Water: In Vivo Quantification with Ultrashort Echo-Time MR Imaging. 2008. **10.** Li, C., et al, Cortical Bone Water Concentration: Dependence of MR Imaging Measures on Age and Pore Volume Fraction. 2014.

Image Results

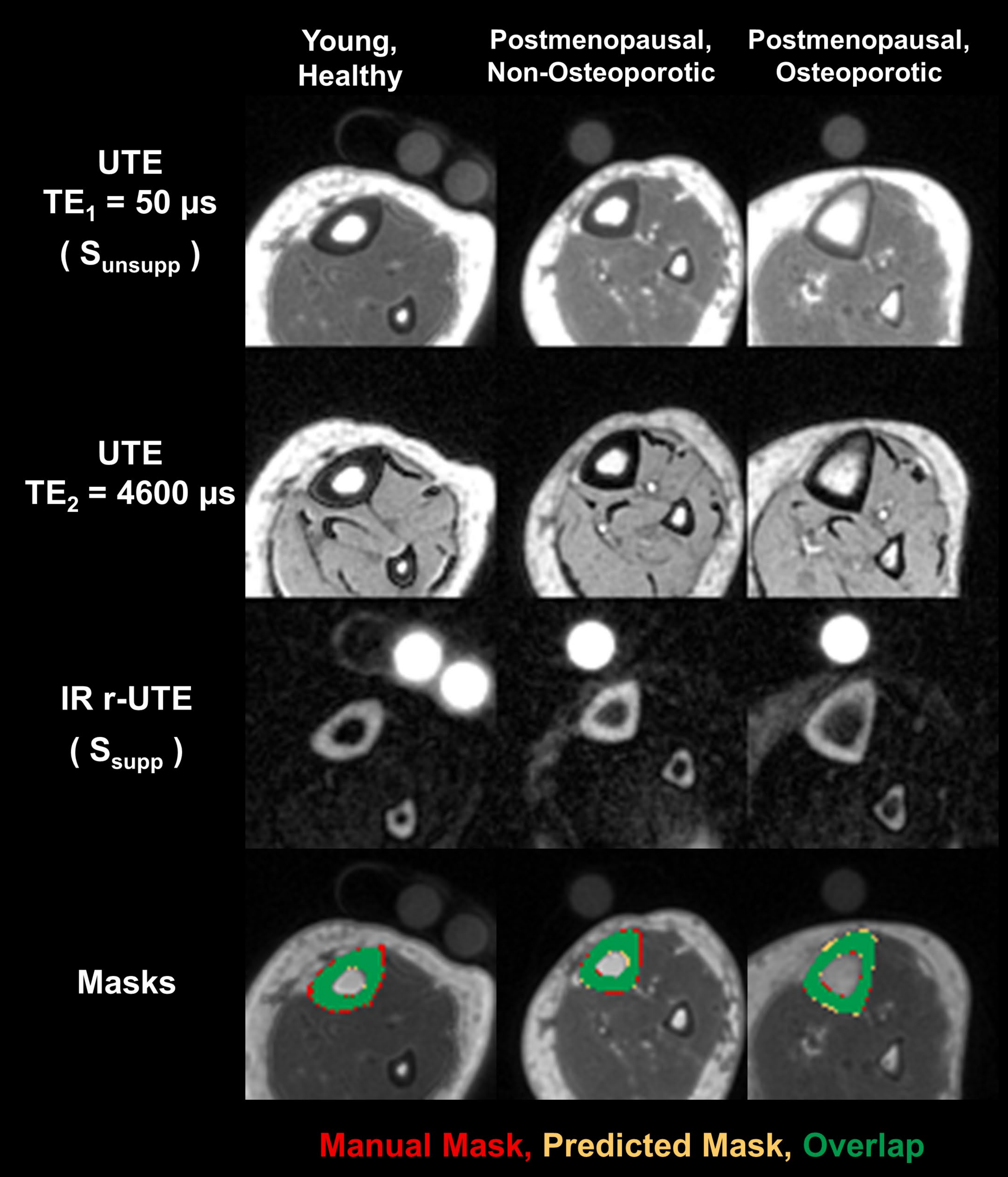

Figure 1: Representative images compared between the three groups. The bottom row displays segmentation accuracy. Green indicates overlapping voxels labeled between manual segmentation and model prediction, whereas red were solely from manual labeling, and yellow were solely from model prediction.

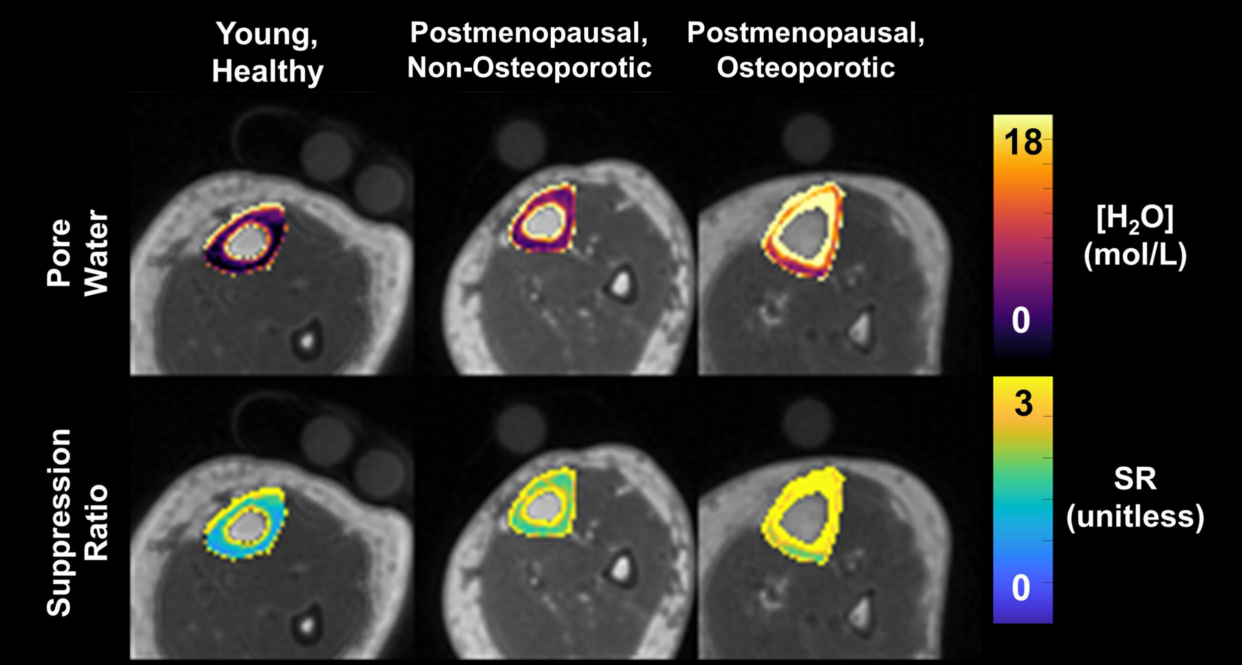

Figure 2: Representative colored porosity parameter maps displayed for the same participants shown at the top. Note the spatial agreement between the porosity parameters of Pore Water and Suppression Ratio, with increasing porosity with age and with osteoporosis.

Segmentation Accuracy

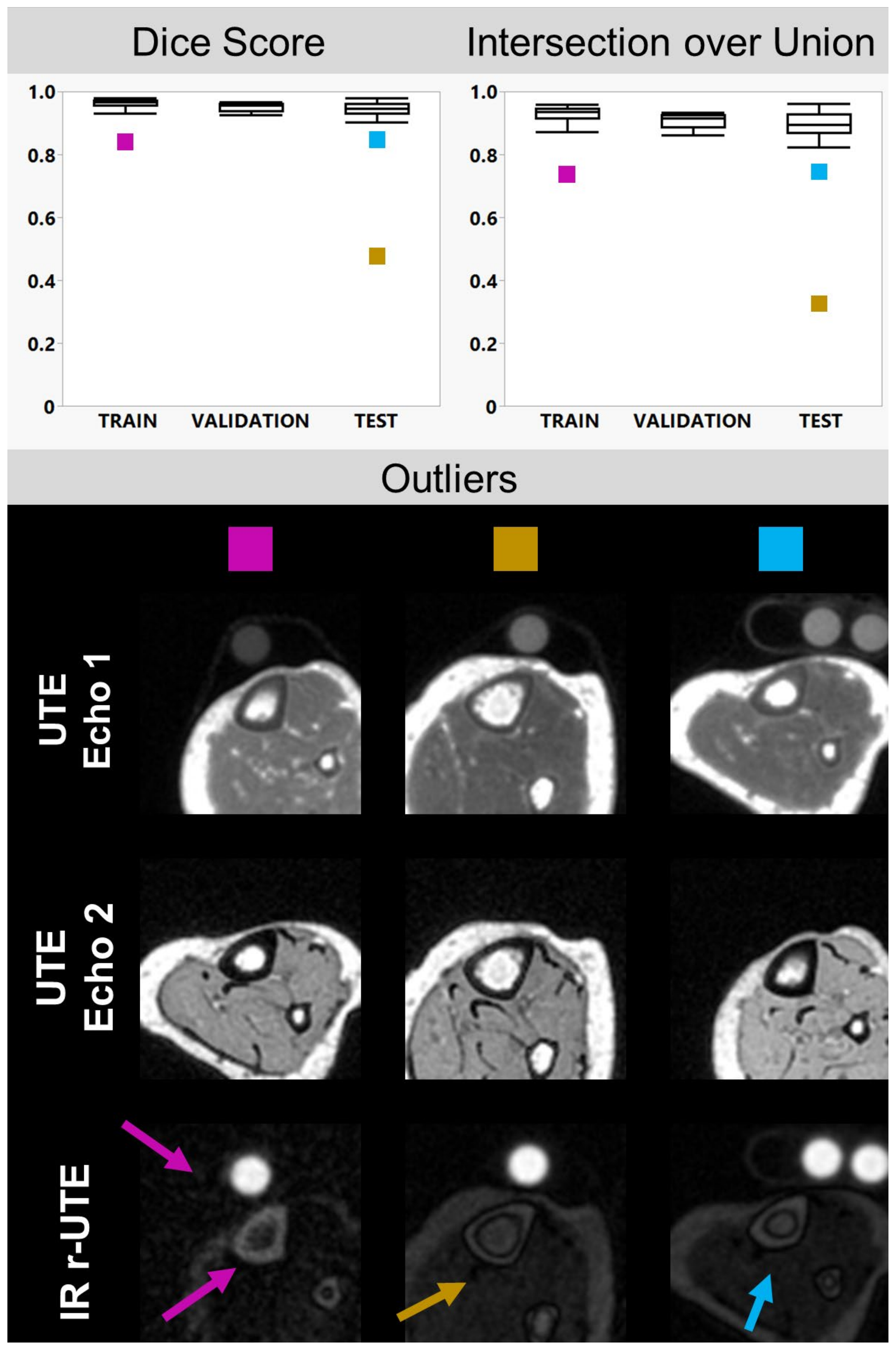

Figure 3: Segmentation accuracy for deep learning segmentation. Note the three outliers plotted as colored boxes, with their corresponding images displayed below. The pink arrows show clear motion artifacts while the other two depict scanning failures in the IR-UTE sequences.

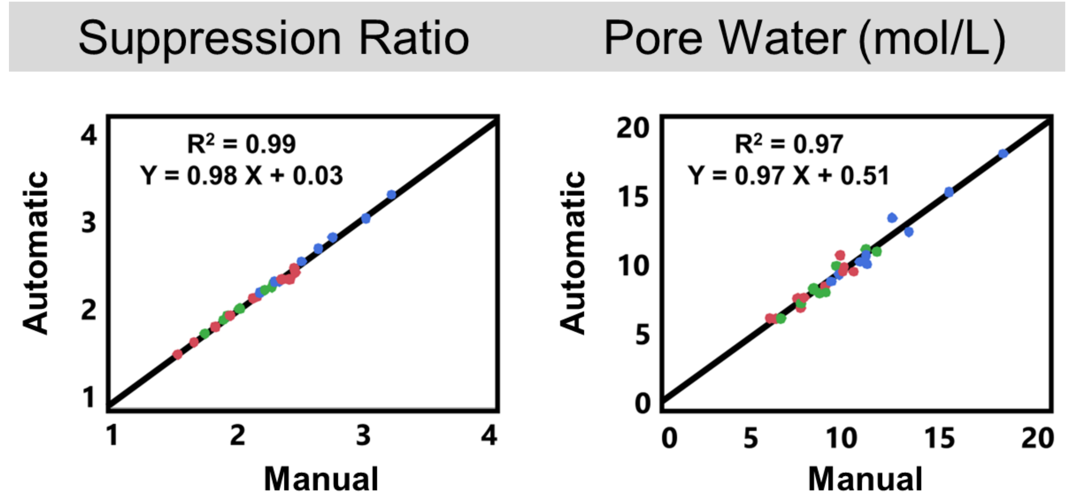

Figure 4: Associations between cortical bone porosity biomarkers obtained from manual segmentations and from automated deep learning segmentations.

Test Dataset / External Validation